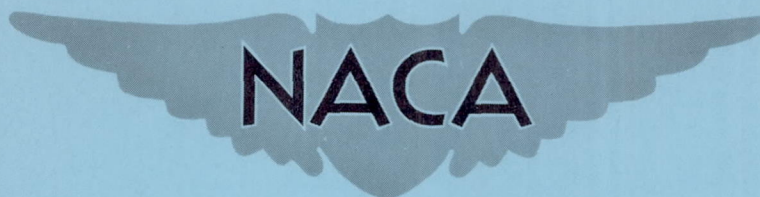# NACA

RESEARCH MEMORANDUM

THE EFFECTS ON THE AERODYNAMIC CHARACTERISTICS OF REVERSING

THE WING OF A TRIANGULAR WING-BODY COMBINATION AT

TRANSONIC SPEEDS AS DETERMINED BY

THE NACA WING-FLOW METHOD

By James M. McKay and Albert W. Hall

Langley Aeronautical Laboratory
Langley Field, Va.

NATIONAL ADVISORY COMMITTEE
FOR AERONAUTICS

WASHINGTON
October 22, 1951

NATIONAL ADVISORY COMMITTEE FOR AERONAUTICS

RESEARCH MEMORANDUM

THE EFFECTS ON THE AERODYNAMIC CHARACTERISTICS OF REVERSING

THE WING OF A TRIANGULAR WING-BODY COMBINATION AT

TRANSONIC SPEEDS AS DETERMINED BY
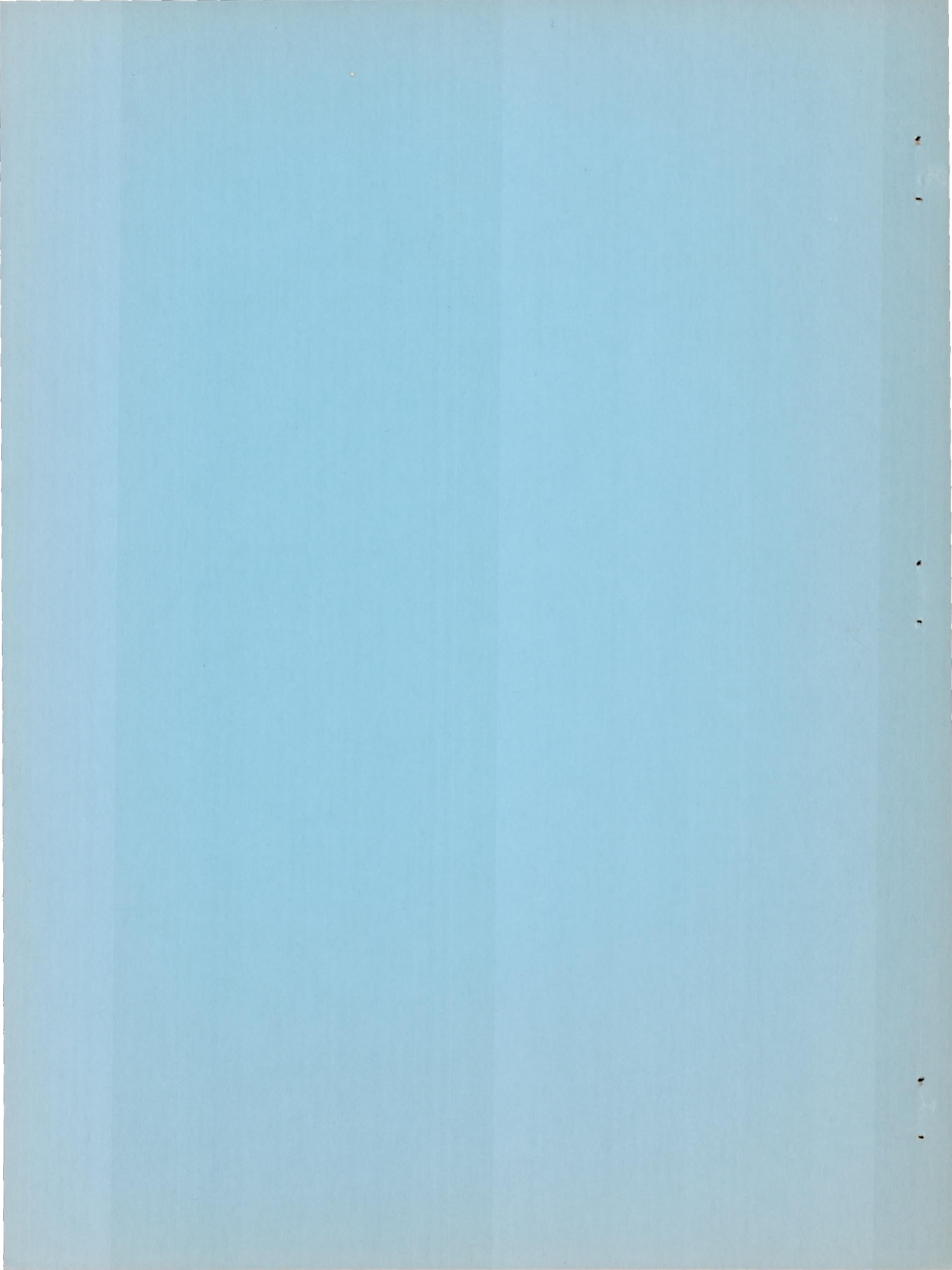
THE NACA WING-FLOW METHOD

By James M. McKay and Albert W. Hall

SUMMARY

Tests were made by the NACA wing-flow method at Mach numbers from 0.75 to 1.075 to determine the effect on the aerodynamic characteristics of reversing a triangular wing with a 6-percent-thick biconvex section. The wing was mounted in combination with a fuselage of fineness ratio 12.

Measurements were made of normal force, chord force, pitching moment, and angle of attack as the model was oscillated through an angle-of-attack range from about -3° to about 10°. The Reynolds number of the tests was approximately 1.5×10^6.

Of the two configurations tested, the wing-reversed combination (apex angle trailing) gave higher lift-curve slopes than the wing-forward configuration (apex angle forward), particularly at the higher Mach numbers. The drag rise at zero lift was slightly delayed for the wing-reversed configuration but the magnitude of the drag rise was about 20 percent greater with the wing reversed than with the wing forward. At zero lift and at low Mach numbers the aerodynamic center for the wing-forward configuration was at approximately the 35-percent mean-aerodynamic-chord position, whereas the aerodynamic center for the wing-reversed configuration was practically at the leading edge of the wing.

INTRODUCTION

As part of a program to determine the effect of wing section, plan form, and thickness on the aerodynamic characteristics of triangular

wings at transonic and low-supersonic speeds, several wing-fuselage con-
figurations have been tested by the NACA wing-flow method. A previous
report, reference 1, presented the effect of section shape on the aero-
dynamic characteristics of two triangular wings. The present paper pre-
sents the effects on the aerodynamic characteristics at transonic speeds
of reversing a triangular wing with a 6-percent-thick biconvex section.
The triangular wing was mounted in combination with a symmetrical fuse-
lage of fineness ratio 12. Measurements were made of normal force, chord
force, pitching moment, and angle of attack as the model was oscillated
through an angle-of-attack range from about -3° to about 10°. The tests
covered a range of Mach numbers from 0.75 to 1.075. The Reynolds number
of the tests was approximately 1.5×10^6, based on the mean aerodynamic
chord of the model.

SYMBOLS

M_L local Mach number at surface of test section

M effective Mach number at wing of model

q effective dynamic pressure at wing of model, pounds
                 per square foot

R Reynolds number, based on mean aerodynamic chord of
                 model

α angle of attack of model wing, degrees

S semispan wing area of model, square feet

b span of model wing, inches

c local wing chord of model, inches

$\bar{c}$ mean aerodynamic chord of model wing, inches $\left(\dfrac{\displaystyle\int_0^{b/2} c^2\,dy}{\displaystyle\int_0^{b/2} c\,dy} \right)$

y spanwise coordinate, inches

L   lift, pounds

M   pitching moment about 50 percent $\bar{c}$ point, inch-pounds

D   drag, pounds

C_L lift coefficient (L/qS)

C_m pitching-moment coefficient $(M/qS\bar{c})$

C_D drag coefficient (D/qS)

$C_{D_{min}}$ minimum drag coefficient

$dC_L/d\alpha$ rate of change of lift coefficient with angle of attack

$\Delta C_D/\Delta C_L^2$ average ratio of the increment of drag coefficient above
                the minimum to the square of the increment of lift
                measured from that corresponding to minimum drag coef-

                ficient $\left(\dfrac{C_D - C_{D_{min}}}{\left[C_L - \left(C_L \text{ at } C_{D_{min}} \right) \right]^2} \right)$

dC_m/dC_L rate of change of pitching-moment coefficient with lift
                coefficient

APPARATUS AND TESTS

The tests were made as described in reference 2 by the NACA wing-
flow method, in which the model was mounted in the region of high-speed
flow over the wing of a North American F-51D airplane.

The triangular wing was made of duralumin and had a 6-percent-thick
biconvex section and a 30° half-apex angle. The fuselage was a half body
of revolution of fineness ratio 12 and was fitted with an end plate. One
configuration had the wing forward (apex angle forward) and the other con-
figuration had the wing reversed (apex angle trailing). The geometric
characteristics of the model are shown in tables I and II and figures 1
and 2. For the wing-forward configuration the wing was mounted on the
fuselage as shown in figure 2. The included area to the fuselage center
line of this arrangement resulted in an aspect ratio of 2.31 with the
mean-aerodynamic-chord location and other dimensions as shown in figure 2
and table I. For the wing-reversed configuration the same wing was

reversed on the fuselage as shown in figure 2. The reversed-wing position was such that the included wing area to the fuselage center line was less than the area for the wing-forward position and the span increased slightly resulting in an aspect ratio of 2.49 and a new mean-aerodynamic-chord length and location as shown in figure 2 and table I.

The models were mounted about 1/16 of an inch above the surface of the test section and fastened to a strain-gage balance below the test section by means of a shank which passed through a hole in the surface. The model and balance oscillated together, thus allowing normal force, chord force, and pitching moment to be measured at various angles of attack.

The chordwise distribution of local Mach number M_L along the airplane wing surface in the test region is shown in figure 3 for several values of airplane Mach number and lift coefficient. The local Mach number was determined from static-pressure measurements made with orifices flush with the surface, in tests with the model removed. The vertical Mach number gradient, determined from measurements made with a static pressure tube located at various distances above the surface of the test section, was found to be 0.009 per inch. The effective Mach number M at the wing of the model was determined as an average Mach number over the wing area of the model. A more detailed discussion of the determination of effective Mach number and effective dynamic pressure q at the model wing can be found in reference 2.

The angle of attack was determined from measurements of model angle and local flow angle. The local flow angle was measured by means of a free-floating vane mounted outboard of the model station as discussed in reference 2.

Continuous measurements were made of normal force, chord force, pitching moment, and angle of attack of the model as the North American F-51D airplane was dived to obtain a range of effective Mach numbers from 1.075 to 0.750. The variation of Reynolds number with Mach number during the dive is shown in figure 4. During the dive the model was oscillated through an angle-of-attack range from about -3° to about 10°.

REDUCTION OF DATA

Lift, drag, and pitching-moment coefficients are based on the wing area extended to the fuselage center line as shown in figure 2. Pitching moments are referred to the 50-percent mean-aerodynamic-chord point for both arrangements tested.

Corrections have been made to the drag for the effect of buoyancy on the fuselage due to pressure gradients in the test region. Buoyancy on the wing for the two arrangements tested was found to be negligible. No attempt has been made to correct the drag data for the effect of the fuselage end plate. Aeroelastic effects were considered negligible and no corrections were applied.

A typical sample of the data for one oscillation of the model through the angle-of-attack range is shown in figure 5. The Mach number during the cycle varied from 0.831 to 0.819, and the curves faired through these points were used to give results for a Mach number of 0.825. Similarly, several cycles were computed for each arrangement and cross-plotted to show the variation of the characteristics with Mach number at constant lift coefficients.

RESULTS AND DISCUSSION

Lift Characteristics

The variation of angle of attack with lift coefficient for several values of Mach number is shown in figure 6 for the two configurations tested. The curves for the wing-reversed configuration indicate an earlier stalling tendency at subsonic speeds than is indicated for the wing-forward configuration. The variation of angle of attack α with Mach number M for several values of lift coefficient C_L is shown in figure 7 for the two configurations tested. The curves presented for the wing-forward combination indicate less variation of angle of attack with Mach number at constant values of lift coefficient than is indicated for the configuration with the wing reversed.

The average lift-curve slopes $dC_L/d\alpha$ for the two configurations over a range of lift coefficients from 0 to 0.3 are shown in figure 8 as a function of Mach number. The values of $dC_L/d\alpha$ for the wing-reversed combination were higher than the values for the wing-forward configuration, particularly at the higher Mach numbers. The lift-curve slope computed according to reference 4 agrees quite well with the measured values throughout the subsonic range for the wing-forward configuration. The lift-curve slope computed according to the method of reference 5 agrees closely with the measured values at Mach numbers above 1.00 for the wing-reversed configuration. The reversibility theorem of linearized theory, reference 3, states that reversing the wing should have no effect on the lift-curve slope. There are many factors involved in the present tests that could cause this difference between the test results and theory. The theorem of reference 3 is based on the wing alone, whereas the present

results contain the effects of fuselage interference, small pressure gradients, and the test-section boundary layer, and other effects peculiar to this type of test procedure.

Drag Characteristics

The variation of drag coefficient C_D with M at constant C_L is shown in figure 9 for the two wing-fuselage configurations. It is believed that the absolute values of C_D for the two configurations are considerably high, because of the drag of the end plate and unknown effects of the semispan method of testing, but the drag rise (increase in drag from subsonic to supersonic values) is believed to be of the correct order. The drag rise seems to occur at a slightly higher Mach number with the wing reversed, particularly at the higher lift coefficients, but the magnitude of the drag rise is approximately 20 percent greater with the wing reversed.

The drag due to lift $\Delta C_D / \Delta C_L^2$ for a range of lift coefficients from 0 to 0.3 is shown in figure 10 as a function of Mach number for the two configurations. The drag due to lift was somewhat less for the wing-reversed configuration at the higher Mach numbers, but was about the same for both configurations at lower Mach numbers.

Pitching-Moment Characteristics

The variation of pitching-moment coefficient C_m with M at constant C_L values is shown in figure 11 for the two wing-fuselage configurations. The aerodynamic-center locations were determined from the slopes dC_m / dC_L of the pitching moment curves at $C_L = 0$ and $C_L = 0.3$, and are shown in figure 12 for the two configurations as a function of Mach number. At $C_L = 0$ and at the lower Mach numbers, the aerodynamic center for the wing-forward configuration is at approximately the 35-percent mean-aerodynamic-chord position, whereas the aerodynamic center for the wing-reversed configuration is practically at the leading edge of the wing. Both configurations show a rearward shift in the aerodynamic center of about 10 percent of the mean aerodynamic chord with an increase in Mach number, the greater part of which occurs at Mach numbers between 0.95 and 1.00. Increasing the lift coefficient to 0.3 had little effect on the location of the aerodynamic center for the wing-forward configuration. With the wing reversed, increasing the lift coefficient to 0.3 moves the aerodynamic center about 10 percent farther rearward at subsonic speeds, but this difference becomes smaller with increase in Mach number.

CONCLUDING REMARKS

Tests were made by the NACA wing-flow method on a triangular wing-fuselage model with a 6-percent-thick biconvex section. Two configurations were tested, one with the wing forward (apex angle forward), and the other with the wing reversed (apex angle trailing), at Mach numbers between 0.750 and 1.075.

The results showed that with the wing reversed, higher lift-curve slopes were indicated than with the wing forward, particularly at the higher Mach numbers. The drag rise at zero lift was slightly delayed for the wing-reversed configuration, but the magnitude of the drag rise was about 20 percent greater with the wing reversed than with the wing forward. The drag due to lift was somewhat less for the wing-reversed configuration at the higher Mach numbers, but was about the same for both configurations at lower Mach numbers. At zero lift and at low Mach numbers the aerodynamic center for the wing-forward configuration was at approximately the 35-percent mean-aerodynamic-chord position, whereas the aerodynamic center for the wing-reversed configuration was practically at the leading edge of the wing.

Langley Aeronautical Laboratory
    National Advisory Committee for Aeronautics
        Langley Field, Va.

REFERENCES

1. Hall, Albert W., and McKay, James M.: Comparison of Airfoil Sections on Two Triangular-Wing-Fuselage Configurations at Transonic Speeds from Tests by the NACA Wing-Flow Method. NACA RM L51F01, 1951.

2. Johnson, Harold I.: Measurements of Aerodynamic Characteristics of a 35° Sweptback NACA 65-009 Airfoil Model with $\frac{1}{4}$-Chord Plain Flap by the NACA Wing-Flow Method. NACA RM L7F13, 1947.

3. Brown, Clinton E.: The Reversibility Theorem for Thin Airfoils in Subsonic and Supersonic Flow. NACA Rep. 986, 1950. (Formerly NACA TN 1944.)

4. DeYoung, John: Theoretical Additional Span Loading Characteristics of Wings with Arbitrary Sweep, Aspect Ratio, and Taper Ratio. NACA TN 1491, 1947.

5. Brown, Clinton E.: Theoretical Lift and Drag of Thin Triangular Wings at Supersonic Speeds. NACA Rep. 839, 1946. (Formerly NACA TN 1183.)

TABLE I

GEOMETRIC CHARACTERISTICS OF MODEL CONFIGURATIONS

	Wing forward	Wing reversed
Wing:		
Section	Biconvex	Biconvex
Thickness ratio, percent chord	6	6
$\bar{c}$, inches	4.07	3.87
Semispan area including projected area of wing in fuselage, square inches	10.78	10.44
Aspect ratio	2.31	2.49
Dihedral, degrees	0	0
Incidence, degrees	0	0
Fuselage:		
Section . . . . Modified 65-series body of revolution		
Length, inches	14	14
Maximum diameter at 50 percent length, inches	1.17	1.17
Fineness ratio	12.0	12.0

NACA
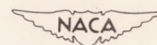
TABLE II

ORDINATES FOR FUSELAGE

[All dimensions are in inches.]

SECTION AA
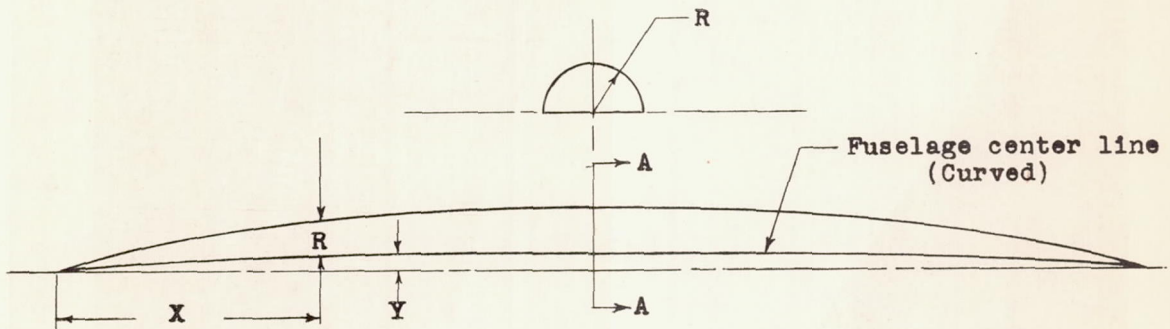
X	Y	R
0	0	0
.070	----	.032
.105	.006	.042
.175	.011	.060
.350	.022	.101
.700	.042	.169
1.050	.059	.226
1.400	.075	.276
2.100	.102	.363
2.800	.124	.433
3.500	.140	.485
4.200	.153	.524
4.900	.160	.551

X	Y	R
5.600	0.169	0.569
6.300	.177	.580
7.000	.188	.583
7.700	.187	.578
8.400	.181	.563
9.100	.171	.538
9.800	.157	.499
10.500	.140	.438
11.200	.124	.354
11.900	.082	.267
12.600	.064	.178
13.300	.035	.089
14.000	0	0

NACA
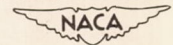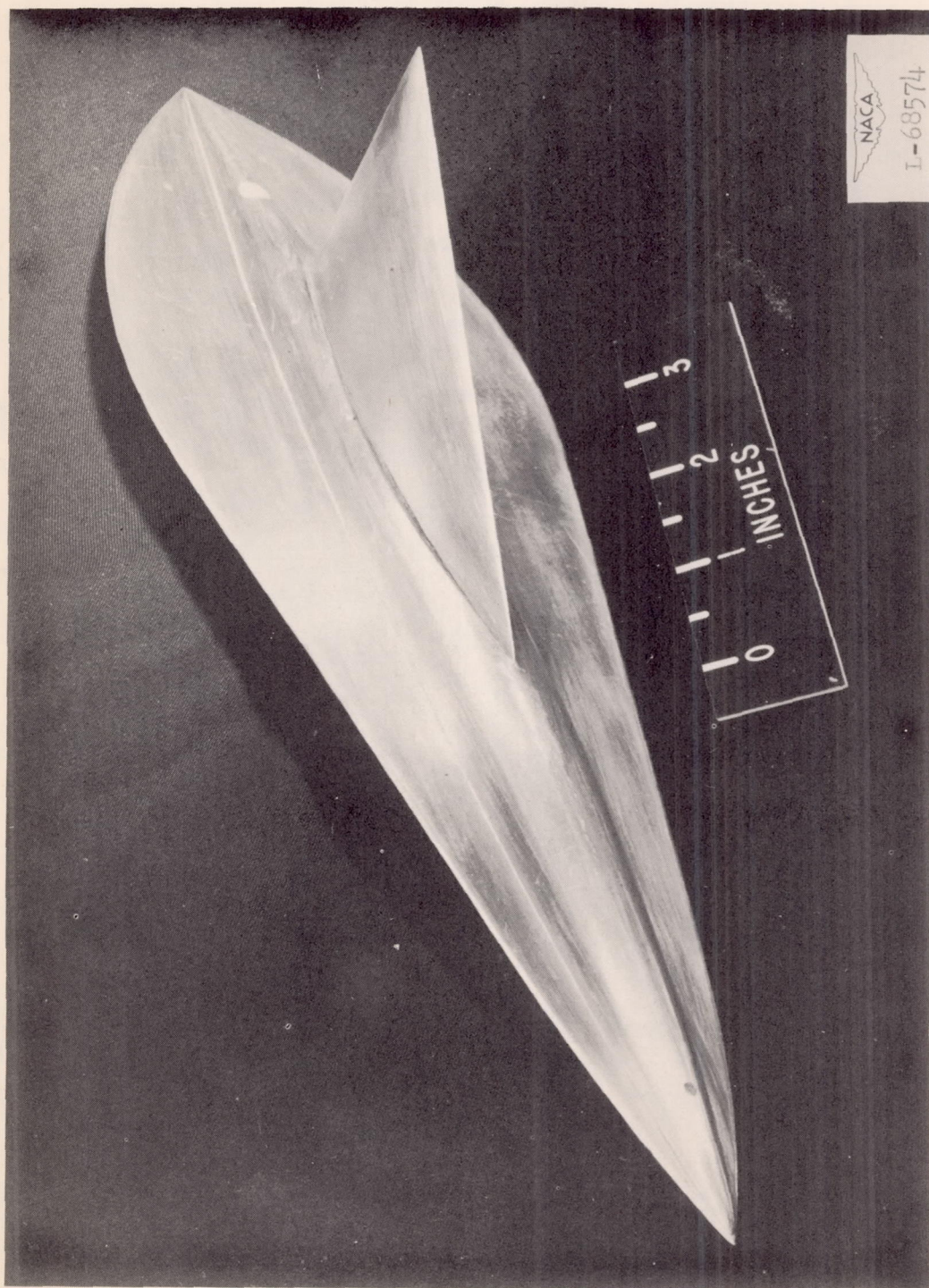
Figure 1.- Semispan wing-fuselage model and end plate (wing-forward configuration).

End plate
Fuselage
(modified 65-series
body of revolution)

1.17

4

14

$\overline{c}$

50%

8.49

Wing forward

30°

3.53

$\overline{c} = 4.07$

$\frac{1}{32}$

$\frac{1}{8}$

F-51D modified
wing surface

6.11

$\overline{c}$

50%

8.92

Wing reversed

3.60

$\overline{c} = 3.87$

NACA

5.80
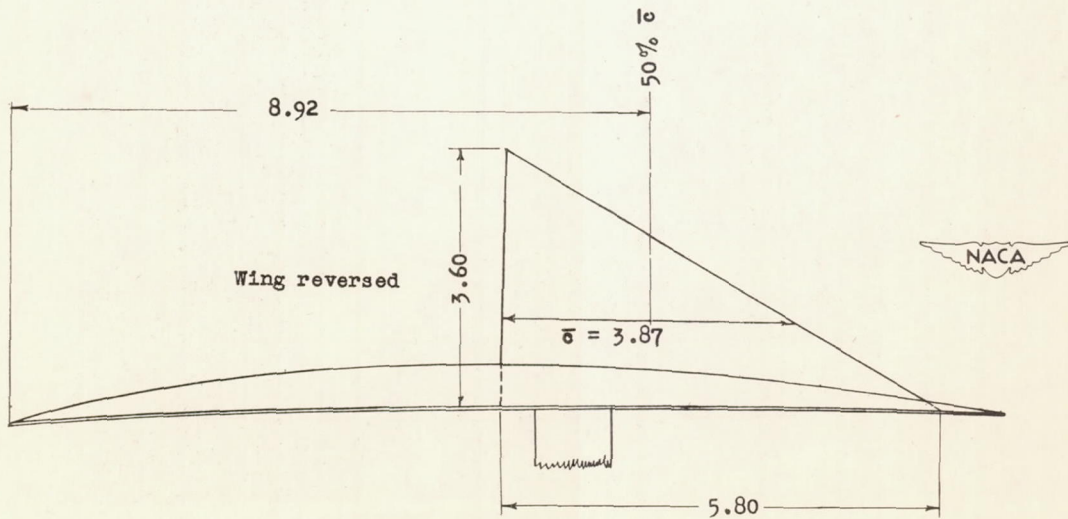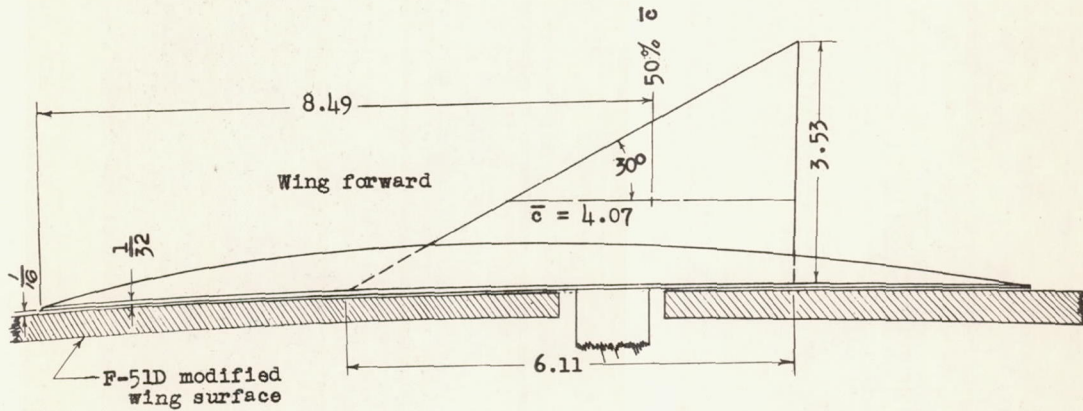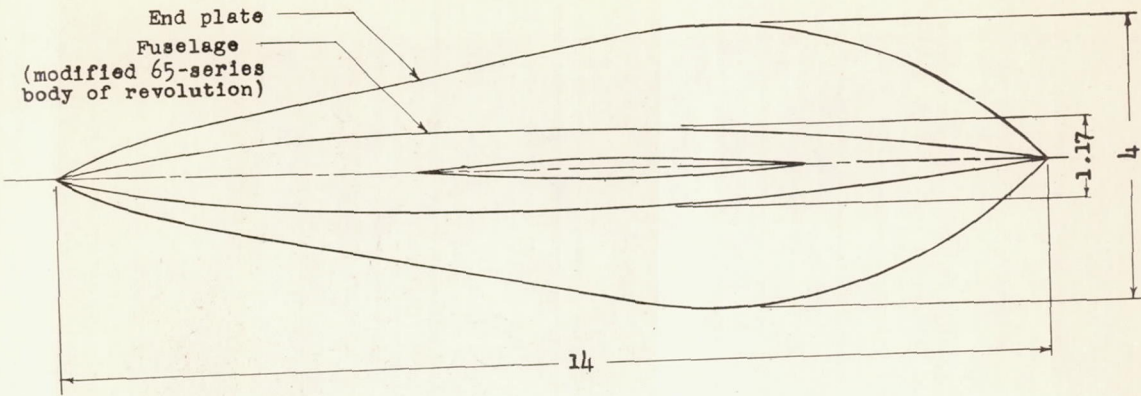
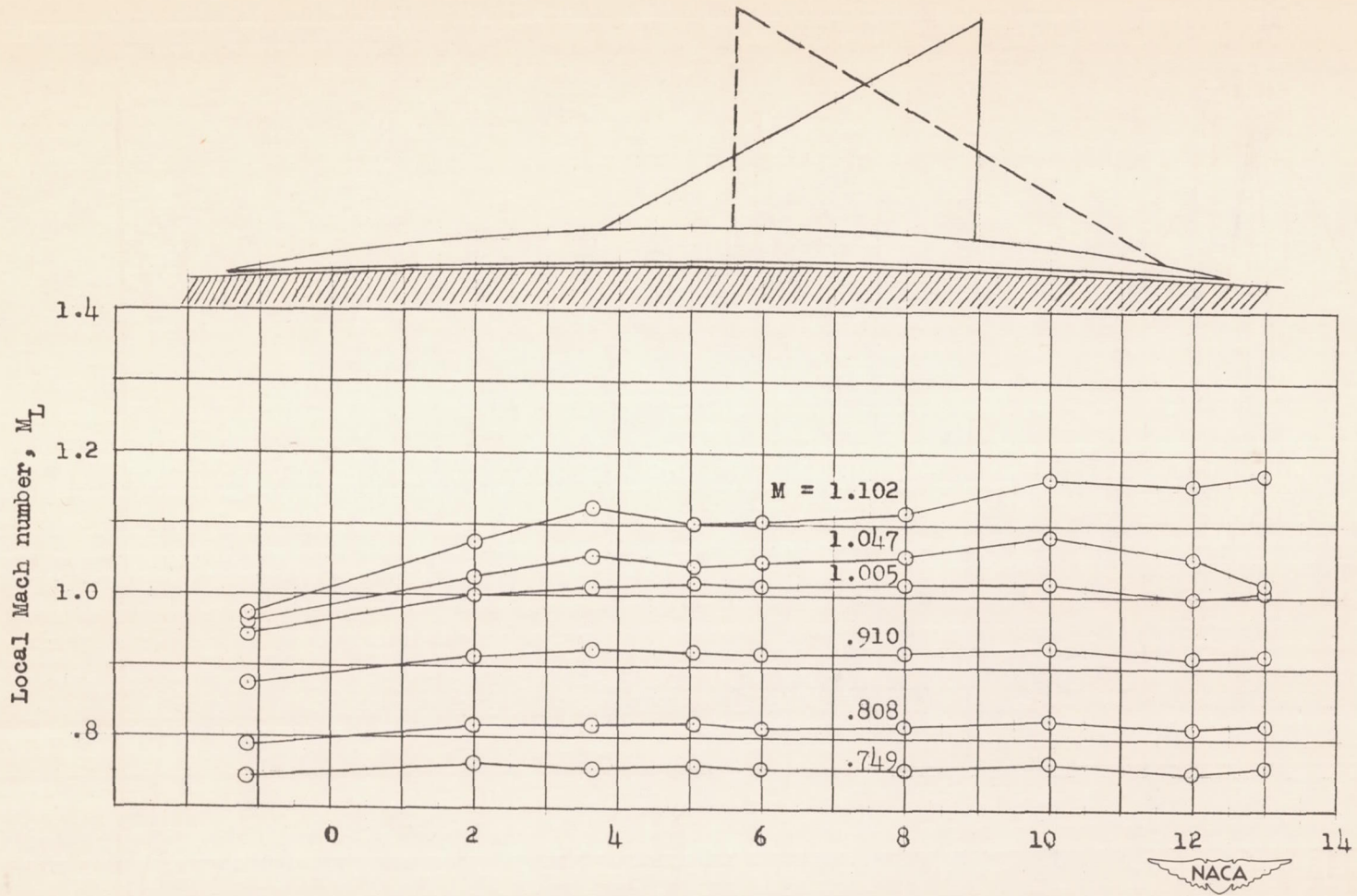Figure 2.- Details of wing-fuselage models. All dimensions are in inches.

Figure 3.- Typical chordwise variation of Mach number in the test region on the surface of the airplane wing for several effective Mach numbers at the wing of the models. Chordwise location of models also shown.
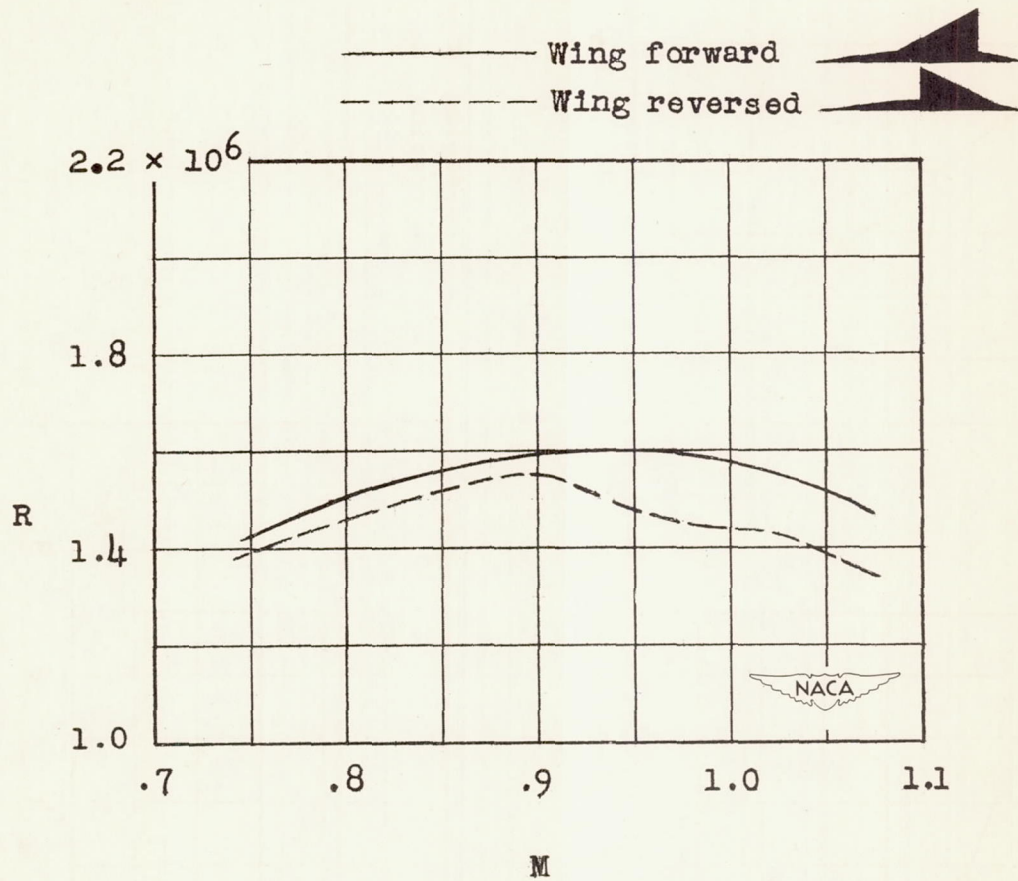
Figure 4.- Variation of test Reynolds number with effective Mach number.
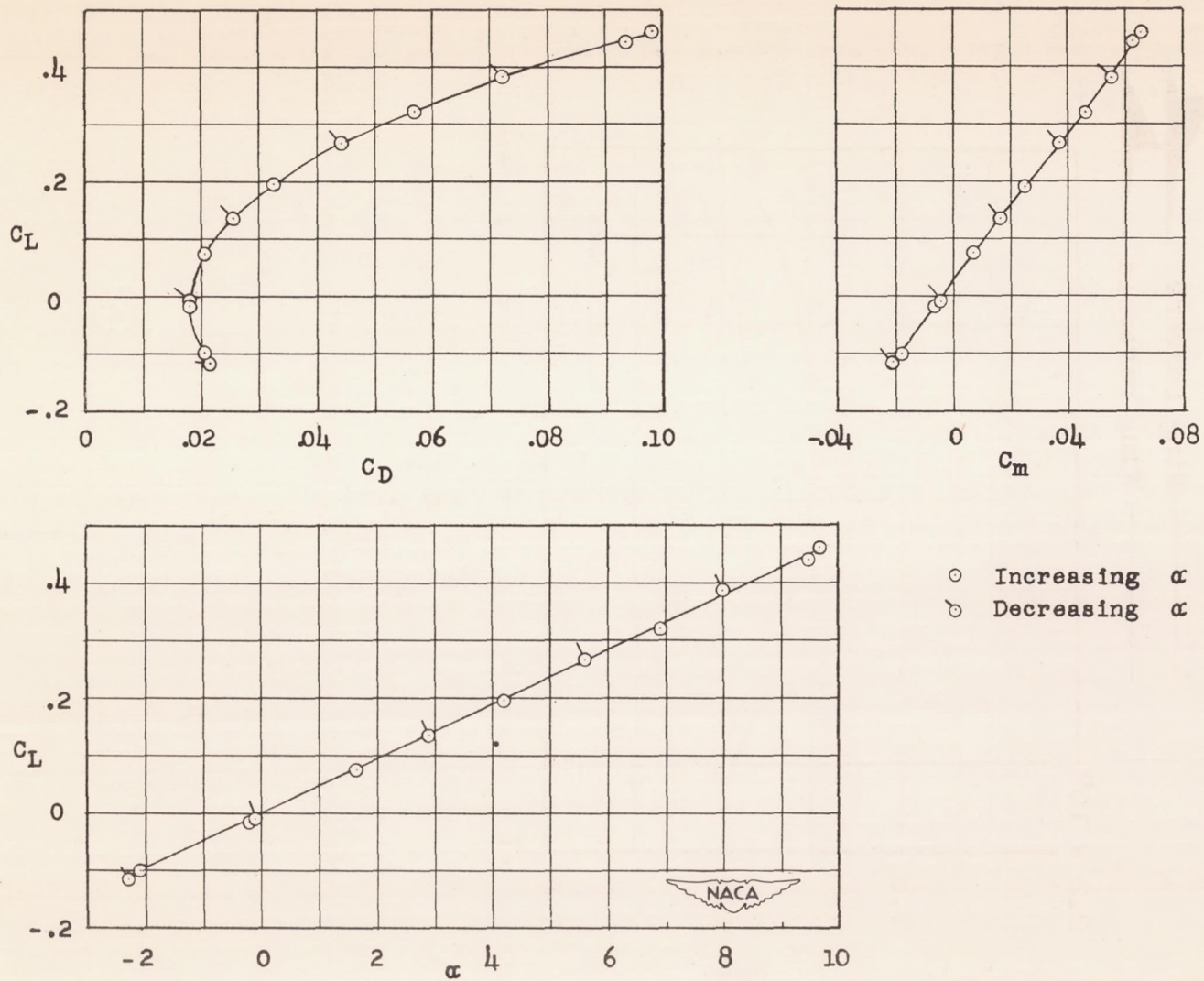
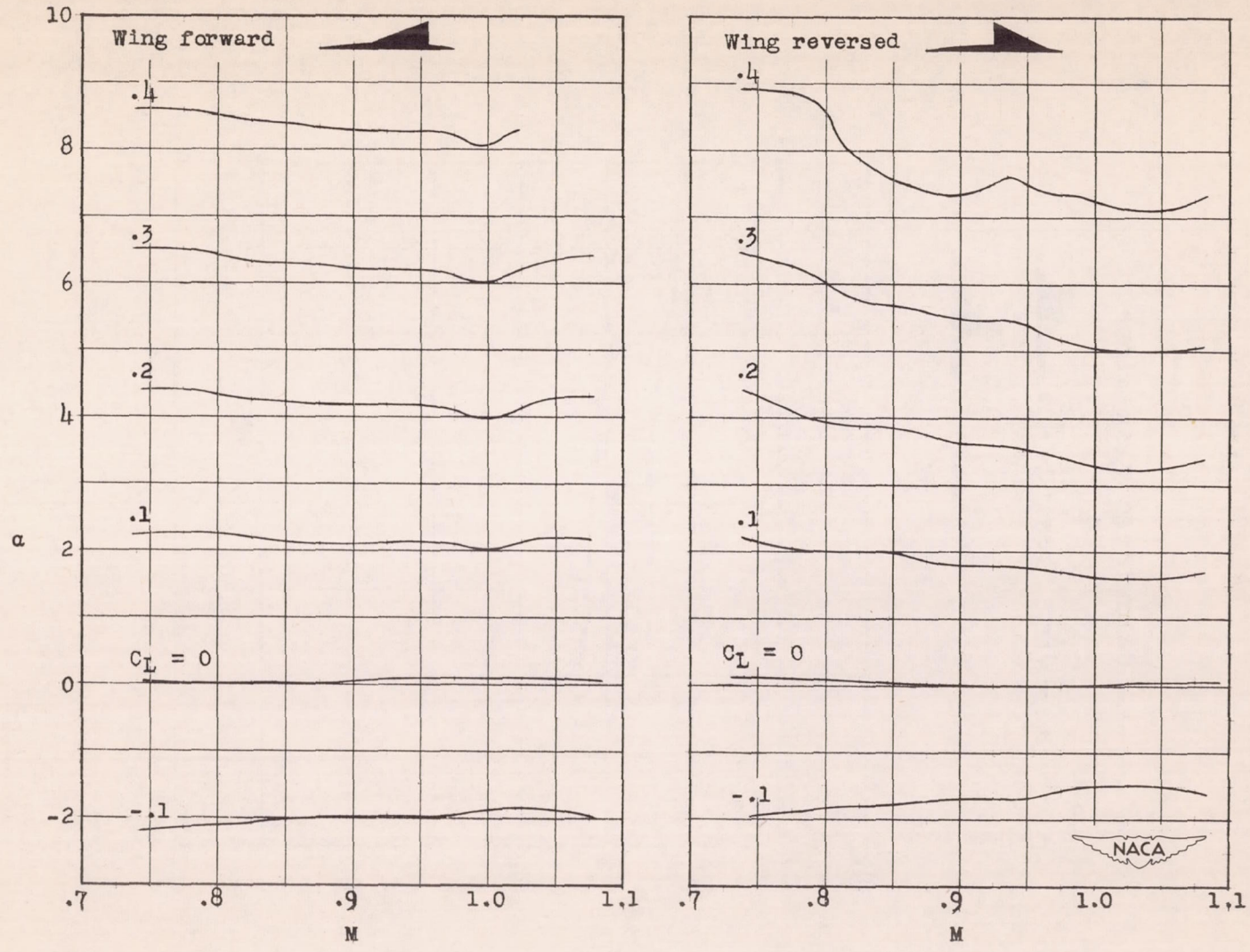Figure 5.- Sample data for wing-fuselage model with wing-forward
configuration. M = 0.825.

Figure 6.- Variation of angle of attack with lift coefficient for
several Mach numbers for the two wing-fuselage configurations.

Figure 7.- Variation of angle of attack with Mach number at constant lift coefficient for the wing-fuselage models.
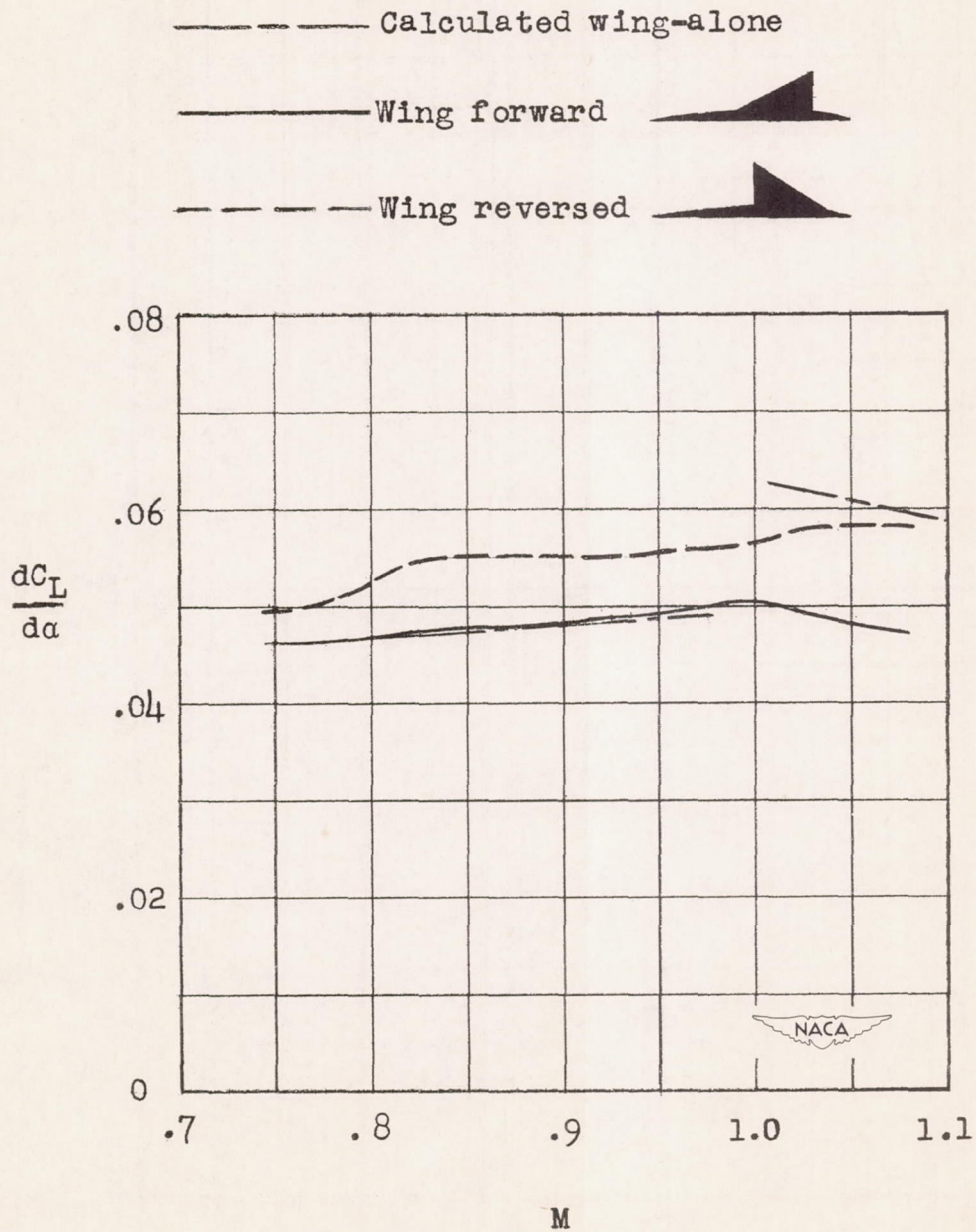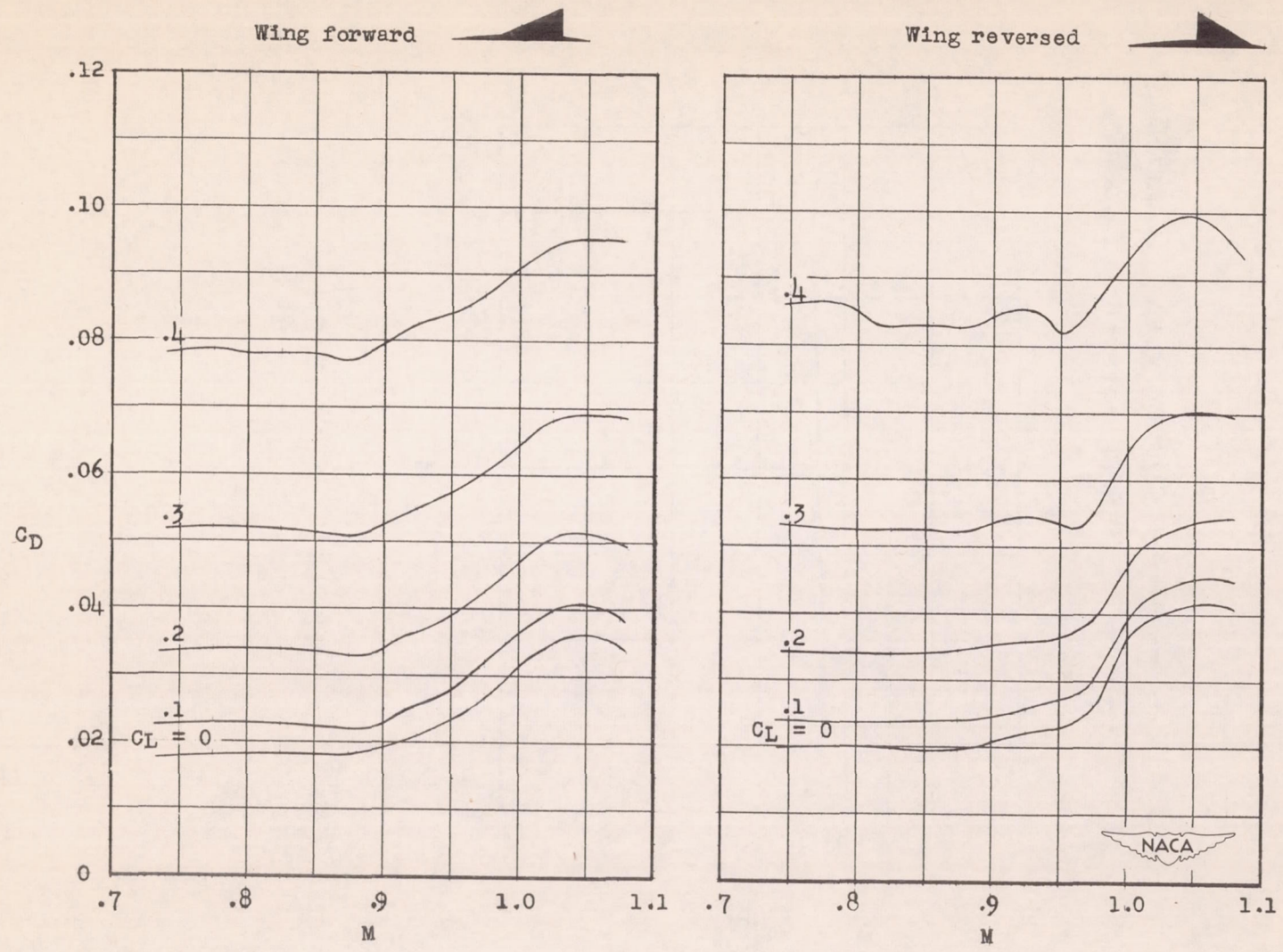
Figure 8.- Effect of Mach number on lift-curve slope of wing-fuselage
configurations.

Figure 9.- Variation of drag coefficient with Mach number at constant
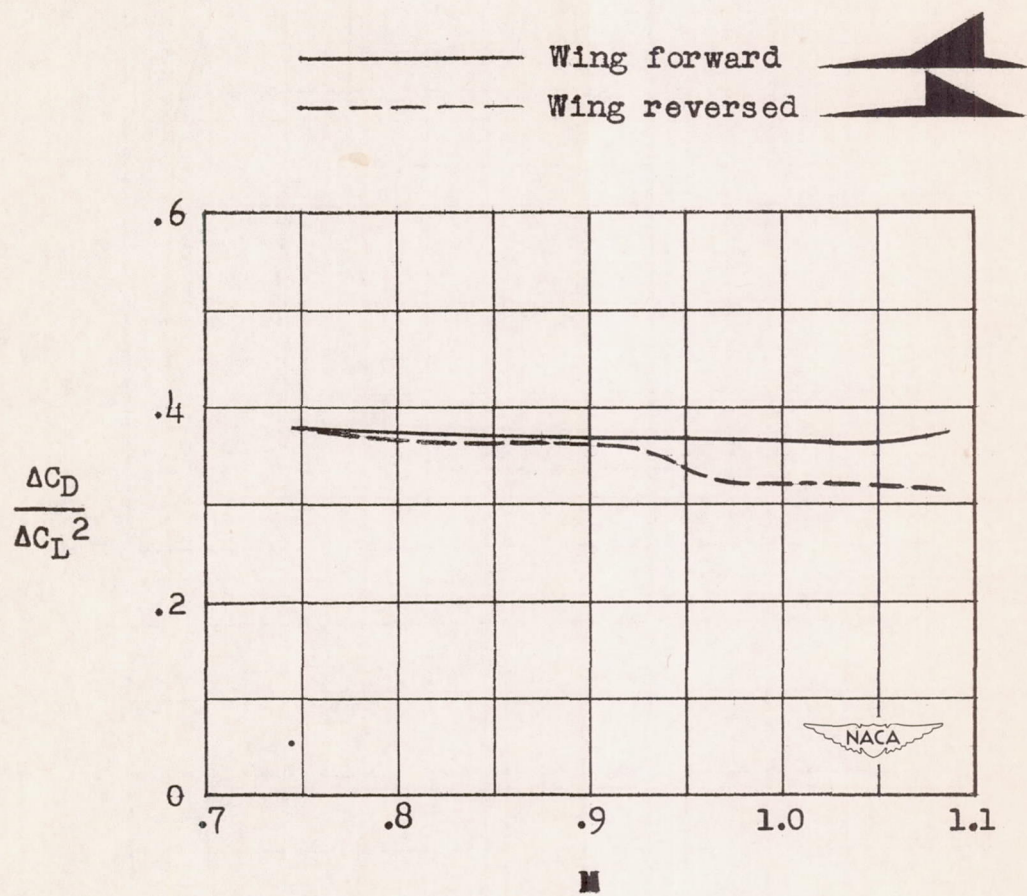lift coefficient for the wing-fuselage configurations.

Figure 10.- Effect of Mach number on $\dfrac{\Delta C_D}{\Delta C_L^2}$.
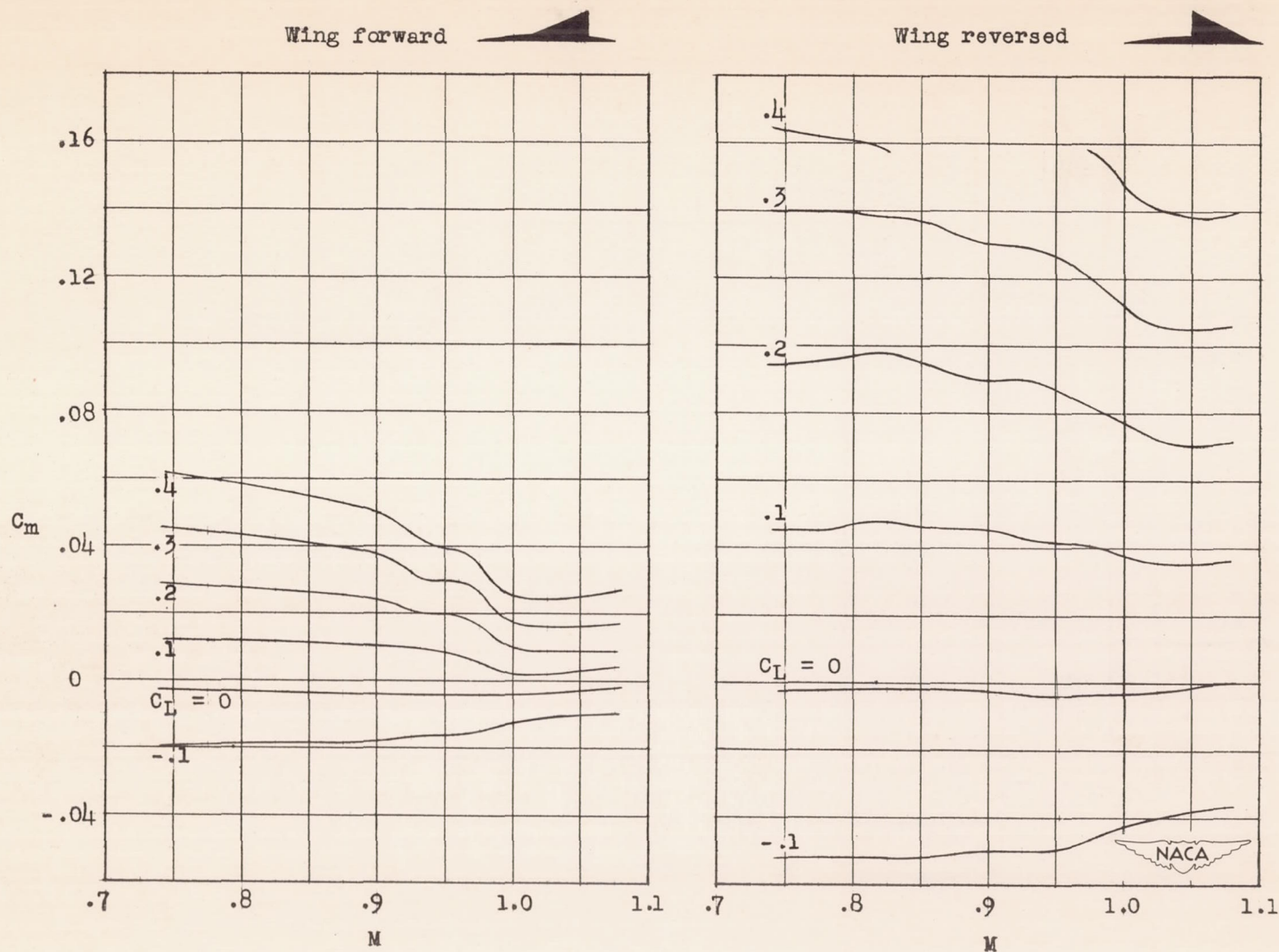
Wing forward

Wing reversed

Figure 11.- Variation of pitching-moment coefficient with Mach number
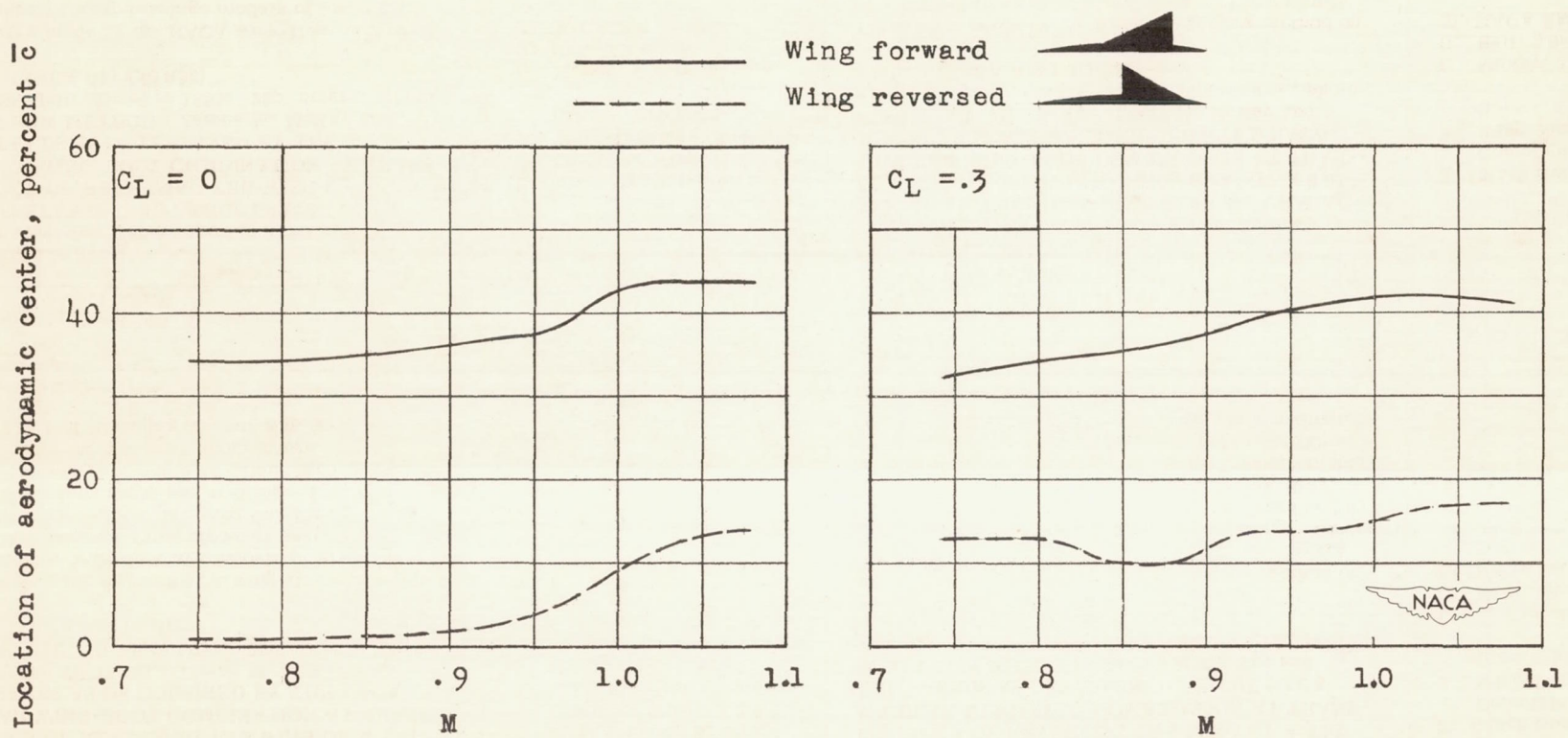at constant lift coefficient for the wing-fuselage models.

Figure 12.- Effect of Mach number on location of the aerodynamic center.